SYNTHESIS, CHARACTERIZATION AND *In-silico* STUDY OF ANTI-CANCER POTENTIAL OF Cu(II) AND Ni(II) COMPLEXES OF (*E*)-2-BENZYLIDENEHYDRAZINECARBOXAMIDE

Aiyelabola, T. O.[*], Fadare, O. A. and Ogundoro, T. J.

[1]The Department of Chemistry, Faculty of Science, Obafemi Awolowo University Ile-Ife, Nigeria.
[*]Corresponding Author's Email: taiyelabola@gmail.com

ABSTRACT

In this study, (*E*)-2-benzylidenehydrazinecarboxamide coordination compounds and mixed ligand metal complexes with oxalic acid or 1,2-diaminocyclohexane were synthesized. Their potential cytotoxic effects and interactions with B-DNA evaluated. This was with a view to demonstrate their potential as anticancer agents for breast cancer. (*E*)-2-Benzylidenehydrazinecarboxamide (benzaldehyde semicarbazone) coordination compounds of Cu(II) and Ni(II) and mixed ligand metal complexes with oxalic acid and 1,2-diaminocyclohexane were synthesized. The resultant complexes were characterized by physicochemical techniques including melting point measurement, percent metal analysis, solubility, and magnetic susceptibility measurements. Electronic and Fourier transform infrared (FTIR) spectroscopy, were performed to further elucidate the structures of the complexes. The synthesized compounds were examined for their cytotoxic effects and DNA interactions with B-DNA. The results obtained showed that all the ligands used were bidentate ligands. They bound to the metal ions through oxygen and nitrogen atoms. All synthesized compounds showed good cytotoxic activity against brine shrimp nauplii except for the (*E*)-2-benzylidenehydrazinecarboxamide copper(II) complex. All of the metal complexes, with the exception of the (*E*)-2-benzylidenehydrazinecarboxamide coordination copper complex, bound to DNA with moderate binding energies. They favoured conventional hydrogen bonding and hydrophobic interaction mostly. The copper complex with 1,2-diaminocyclohexane had the most interaction and a good binding effect to the DNA and better than oxaliplatin, the standard used. This therefore indicated the potential of these compounds as probable chemotherapeutic agents against breast cancer cells.

Keywords: (*E*)-2-Benzylidenehydrazinecarboxamide, Oxalic acid, 1,2-Diamonium cyclohexane, Mixed-ligand complexes, B-DNA, Breast cancer.

INTRODUCTION

Breast cancer is the second leading cause of death in women worldwide and one of the most common carcinomas among the many different types of cancer (Katayoon *et al.* 2019). It has recently been reported that in women, it is a silent killer posing a major challenge for the society (Zubair *et al.*, 2023). DNA damage or genetic mutations can lead to the development of breast cancer due to uncontrolled and abnormal cell division. Interestingly, it has been reported that breast cancer is due in large part to genetic mutations that occur as a result of the aging process and lifestyle-related risk factors rather than inherited mutations (Feng *et al.*, 2018). Several chemotherapy drugs have been reported for the treatment of breast cancer using *in vivo* and *in vitro* methods. There are reports of regimens based on metal-based chemotherapy that induces apoptosis in cancer cells (Ana-Maria and Bsselberg, 2011). Among these are platinum-based drugs such as cisplatin, carboplatin, and oxaliplatin. These have been reported as chemotherapeutic agents approved by the US Food and Drug Administration to treat a broad spectrum of cancer cells. It has been reported that these complexes exert their anticancer effects by binding to DNA. This alters cell replication and inhibits the growth of tumor cells (Uri *et al.*, 2020; Aiyelabola *et al.*, 2021). However, side effects such as nephro-, oto- and cardio-toxicity, as well as resistance, represent a major setback for these drugs (Gaynora *et al.*, 2012). Against this background, much attention has been paid to the development of new metal-based complexes as anticancer drugs to minimize side effects. (Tamasi *et al.*, 2008). Semicarbazone and its complexes have been of great interest because of their anti-cancer, -bacterial, -malarial, and -viral effects (Wilfredo *et al.*, 2006; Shahu *et al.*, 2012).

Copper(II) complexes are highly favoured in the literature for their promising chemotherapeutic activity in the treatment of cancer. Furthermore, it

has been reported that copper complexes with N-donor ligands have good binding affinity to nitrogenous DNA base and better binding mode with DNA through intercalation, hydrogen bonding and groove binding, resulting in blocking of DNA replication (Wende *et al.*, 2014). It was also reported that the nickel(II) complex showed good DNA binding affinity with 1BNA at the major groove, but the copper(II) complex showed stronger hydrogen bonding and binding affinity compared to the nickel(II) complex (Icsel *et al.*, 2020). Molecular docking has gained great interest today due to the fact that they are affordable, as well as their ability to evaluate and elucidate interaction between potential ligands, metal-based drugs and their macromolecular targets. As a consequence, it may assist in the discovery of new

drugs to occur more rapidly. Therefore, it was considered to design and study coordination complexes of (*E*)-2-benzylidene-hydrazinecarboxamide, with potential minimal side effect than the platinum-based anticancer chemotherapeutics currently in use.

Herein, we describe the synthesis, characterization and DNA binding profile of Cu(II) and Ni(II) complexes of (*E*)-2-benzylidene-hydrazinecarboxamide (**L1**) (Figure 1) as well as its mixed ligand complexes with oxalic acid (**L2**) or 1,2-diaminocyclohexane (**L3**), Figure 1, as potential anticancer agent, for breast cancer. The results obtained from the brine shrimp lethality assay and molecular docking studies with B-DNA are also reported.
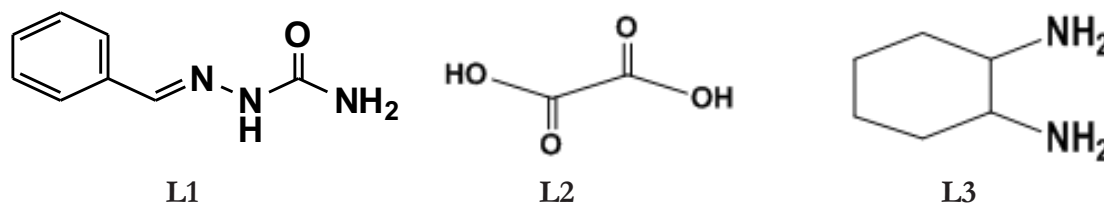
Figure 1: The organic ligands used for metal complexation in this study.

EXPERIMENTAL
Materials
The solvents and reagents used were of analytical grade and were obtained from Sigma-Aldrich Chemical Limited and British Drugs House Chemical Ltd (BDH) and used without further purification. These include semicarbazide hydrochloride, benzaldehyde, sodium acetate, oxalic acid, 1,2-diaminocyclohexane, ethanol, methanol, dimethyl sulfoxide (DMSO), acetone, dimethylformaldehyde (DMF), copper(II) and nickel(II). The seawater used was sourced from Badagry beach (Lagos, Nigeria). The *in-silico* studies were performed using Autodock 4.2, PyMol and Discovery Studio softwares.

Methodology
(*E*)-2-Benzylidenehydrazinecarboxamide (**L1**) was synthesized by a condensation reaction involving the reaction of benzaldehyde and semicarbazide hydrochloride in the presence of sodium acetate. (*E*)-2-Benzylidene-hydrazinecarboxamide coordination complexes were prepared in a 1:2 molar ratio. The mixed ligand complexes were prepared using

benzaldehyde semicarbazone with either oxalic acid (**L2**) or 1,2-diaminocyclohexane (**L3**) in a 1:1:1 molar ratio. Ni(II) and Cu(II) acetate salts were used to obtain the coordination complexes (and the mixed ligand complexes) with the respective ligands to give the desired metal complexes. The synthesized metal complexes were then characterized using spectral measurements, physicochemical measurements (melting point measurement, metal analysis) and magnetic moments. The infrared spectra of all synthesized products were obtained using Agilent Cary 630 FTIR. The electronic spectra, of all the compounds, were obtained in solution, in the wavelength range 400-1000 nm using 1800 Shimadzu ultra-violet spectrophotometer. Magnetic susceptibility measurement of the metal complexes was obtained using a MSB Mk1 magnetic susceptibility balance, Sherwood Scientific with [HgCo(SCN)$_4$] as standard, at the Kwara State University, Ilorin. The metal analyses for the complexes were obtained using titrimetric method using EDTA. The brine shrimp lethality test was performed on the metal complexes, and *in silico* studies of DNA binding ability were

performed using molecular docking. A synthetic scheme for the preparation of **L1** and all complexes is depicted in Figure 2.

Synthesis of (*E*)-2-benzylidenehydrazinecarboxamide

Semicarbazide hydrochloride (1.15 g, 0.001 mol) and sodium acetate (0.82 g, 0.001 mol) were weighed and dissolved in 25 mL of distilled water in a 250 mL beaker and set up to stir. Benzaldehyde 1.06 mL (1.11 g, 0.001 mol) was added to the stirring solution after which the reaction mixture was heated to 70 °C and left to stir for 15 minutes. The solution obtained was allowed to cool and this afforded a white precipitate (the semicarbazone) which was separated from the solution by filtration and oven-dried. The melting point and percent yield were determined and recorded.

Syntheses of Metal Complexes
Preparation of Cu-L1
Copper(II) acetate (1.82 g, 0.01 mol) was dissolved in 5 mL of water, and was added to **L1** (1.63 g, 0.01 mol) while stirring. The reaction mixture was left

to stir for 40 min. at 110 °C. The resultant product was left to stand and cool to room temperature to give a green precipitate. The product was obtained by filtration and dried.

Preparation of Ni-L1
Nickel(II) acetate (1.768 g, 0.01 mol) was dissolved in 5 mL of water, **L1,** the (*E*)-2-benzylidenehydrazinecarboxamide (1.63 g, 0.01 mol) while stirring. The mixture was stirred and heated at 110 °C for 40 min. The product obtained was cooled to room temperature, and a white precipitate was obtained. The product was isolated by gravitational filtration and dried.

Preparation of Cu-L1-L2
Copper(II) acetate (1.82 g, 0.01 mol) was dissolved in 5 mL of water, this was added with heating to a mixture (*E*)-2-benzylidenehydrazinecarboxamide (1.63 g, 0.01 mol) and oxalic acid (1.26 g, 0.01 mol) and stirred at 110 °C using a magnetic bar. After cooling a green precipitate was observed. The product was obtained by gravitational filtration and dried.
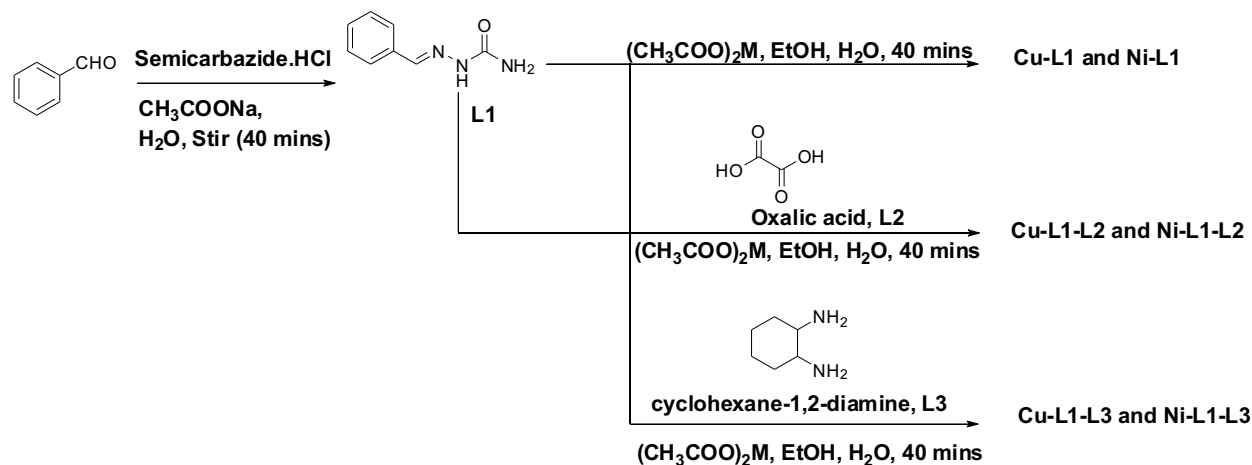
Figure 2: The synthetic scheme for the preparation of L1 and all the metal complexes.

Preparation of Ni-L1-L2
Nickel(II) acetate (0.88 g, 0.005 mol) was dissolved in 5 mL of water, this was added to a mixture of (*E*)-2-benzylidenehydrazinecarboxamide (1.63 g, 0.005 mol) and oxalic acid (0.66 g, 0.005 mol) on heating and stirred at 110 °C using a magnetic bar. The reaction flask was left to stand and cool to room temperature this afforded a white precipitate. The product was obtained by gravitational filtration and dried.

Preparation of Cu-L1-L3
Copper(II) acetate (1.82 g of 0.01 mol) was dissolved in 5 mL of water, this was added to a mixture of (*E*)-2-benzylidenehy drazine-carboxamide (1.63 g, 0.01 mol) and 1,2-diaminocyclohexane (1.09 g, 0.01 mol) heating and stirred at 110 °C using a magnetic bar for 40 min. The resultant mixture was left to stand and cool to room temperature to afford a turquoise blue precipitate. The product was obtained by gravitational filtration and dried.

Preparation of Ni-L1-L3

Nickel(II) acetate (0.884 g, 0.005 mol) was dissolved in 5 mL of water, the solution was added to a mixture (*E*)-2-benzylidenehy drazinecarboxamidee (0.82 g, 0.005 mol) and 1,2-diaminocyclohexane (0.55 g, 005 mol) on heating and stirred at 110 °C using magnetic bar for 45 min. The resultant mixture obtained was left to stand and cool to room temperature which afforded the precipitation of the (tortilla brown) colored complex. The product was obtained by gravitational filtration and dried.

DNA Binding Study (In-silico)

The ability of the metal complexes to bind to DNA was probed by molecular docking calculations. The target DNA was retrieved as crystal coordinates (1BNA) from the protein database. The crystal structure was prepared for docking with the PyMol software, water molecules were removed and the stripped DNA was resaved in the protein data bank (pdb) format. DNA molecule (without associated water molecules) was loaded into the AutoDock tools, where polar hydrogens as well as Gasteiger charges, were added. A grid box with dimensions (Angstrom units), x = 40, y = 40, z = 40 and center coordinates (0.375) was set up around the DNA molecule which was saved in pdbqt format for the docking calculations. The 3D structure of the metal complexes was generated by first drawing in 2D with the MarvinSketch program and saving the files in mol2 format. The 2D structure files were imported into the Avogadro software for optimization and saved in a pdb format ready for docking calculation in the AutoDock program. The optimized 3D structures of the metal complexes were loaded into the AutoDock program and used for the docking calculations. The parameter file for the AutoDock program was edited by including the parameters for the metals before the docking run. The binding affinity estimates for different positions of the complexes with DNA were retrieved after the docking calculations, and the best binding positions (with the highest binding affinity) were selected for viewing and visualization in PyMol and Discovery Studio to obtain the interactions of the metal complexes with DNA.

In vitro cytotoxic studies

Hatching of brine shrimp eggs

The brine shrimp eggs were obtained from the local market and hatched in a glass container of sea water. The glass compartment had two partitions; one was illuminated, and the other part was dark (no light entering). After 24 h of hatching at room temperature, the eggs hatched into larvae (nauplii) that swim toward the illumination chamber, leaving their shells in the dark chamber. The nauplii were carefully collected with a dropper for bioassay.

Preparation of test compounds

From each of the test compound, 32 mg was taken and dissolved in 200 L of dimethyl sulfoxide (DMSO). The concentration of the stock solution was 1600 g/mL. Five samples with a volume of 5 mL and different concentrations of 1000, 800, 600, 400, and 200 g/mL were prepared by diluting the stock solution with sea water. The control group was used to validate the test method and ensure that the measure of lethality was solely due to the activity of the test complexes. As a control, 50 g/mL DMSO in 5 mL seawater without the presence of metal complexes or ligands was used.

Brine Shrimp Lethality Assay

Ten nauplii (larvae) were added to the five different concentrations prepared (1000, 800, 600, 400, 200 μg/mL). After 24 h, the nauplii in each vial were counted with the aid of a 3 × magnifying glass for the surviving brine shrimp. The mortality endpoint of this bioassay was observed based on the absence of controlled forward motion during the 30 s of observation.

RESULTS AND DISCUSSION
Physico-Chemical Characterization

The physical and chemical properties of the (*E*)-2-benzylidenehydrazinecarboxamide coordination complexes include their colour, melting point/decomposition temperature, percentage yield and the percentage metal composition. These are presented in Table 1.

Table 1: Physical properties and analytical data for the ligands and complexes.

Complexes	Molecular weight	Colour	% yield	%Metal found (calculated)	Melting point (°C)
L1	163.169	White	73	NA	218-220
L2	90.034	white	NA	NA	185-187
L3	114.189	Colourless	NA	NA	NA
Cu-L1	815.767[a]	Dark grey	74	7.79 (7.58)	194-197
Ni-L1	384.978[a]	White	67	15.24 (15.8)	214-217
Cu-L1-L2	549.972[a]	Green	66	11.55 (11.32)	214-216
Ni-L1-L2	309.885[a]	White	82	18.94 (18.53)	221-224
Cu-L1-L3	717.806[a]	Turquoise blue	61	8.85 (8.75)	204-207
Ni-L1-L3	335.998[a]	Tortilla brown	58	17.46 (16.79)	217-220

NA = Not applicable (Note: compound L3 is a liquid), a – proposed molecular weight

FT-IR studies

Infrared spectrum of ligands

The infrared spectrum of (*E*)-2-benzylidenehydrazinecarboxamide (**L1**) showed two broad bands at 3459 and 3280 cm^{-1}, attributable to a primary amine vibrational frequency. The weak band at 3246 cm^{-1} indicated the presence of a secondary amine (N-H) vibrational frequency. A strong band at 1643 cm^{-1} indicated the presence of a carbonyl stretching frequency. The sharp band at 1595 cm^{-1} was assigned to the aromatic C=C vibrational frequency, and the weak band at 1509 cm^{-1} was assigned to the C=N vibrational frequency. A comparison of the spectrum of (*E*)-2-benzylidenehydrazinecarboxamide and its starting materials (semicarbazide hydrochloride and benzaldehyde) revealed the appearance of a C=N vibrational frequency at 1509 cm^{-1} in the IR spectrum of (*E*)-2-benzylidenehydrazinecarboxamide which was absent in the other named materials. This, therefore, indicated the formation of the ligand. Furthermore, the absence of the aldehyde-induced carbonyl stretching frequency at 1695 cm^{-1}, characteristic of benzaldehyde, served as further support for the formation of the semicarbazone. A downward shift of the carbonyl vibrational frequency of (*E*)-2-benzylidenehydrazinecarboxamide at 1643 cm^{-1} was observed. On the other hand, the carbonyl vibration frequency in semicarbazide was observed at 1677 cm^{-1}. This confirmed the formation of (*E*)-2-benzylidenehydrazinecarboxamide in addition with the melting point value, which was in agreement with previous report.

The Infrared spectrum of oxalic acid (**L2**) showed a broad peak at 3497 cm^{-1}, which suggested the presence of ν(O-H) vibration frequency. A band at 1720 cm^{-1} indicated the presence of unsaturated carbonyl vibrational frequency of a carboxylic acid.

The spectrum of 1,2-diaminocyclohexane (**L3**) showed two weak bands at 3354 and 3280 cm^{-1}, suggesting the presence of N-H vibrational frequency of a primary amine, characteristic of 1,2-diaminocyclohexane. Two bands at 2922 and 2855 cm^{-1} indicated the presence of ν(C-H) of cyclohexane. The peak at 1446 cm^{-1} suggested CH$_2$ bending vibrational frequency.

Infrared Spectra of the Metal Complexes

The infrared spectra of the metal complexes exhibited similar vibrational frequencies to that of the ligands in many cases, and this is not unexpected. Shifts to higher or lower frequencies were observed in the spectra of the complexes upon which suggested coordination of the metal ion.

Infrared Spectra of copper(II) complexes

The spectrum of Cu-L1 showed broad bands at 3380 and 3283 cm^{-1}, suggesting the presence of primary N-H vibrational frequency. A weak band at 3194 cm^{-1} indicated the presence of a secondary N-H vibrational frequency. The medium intensity band at 1640 cm^{-1} was assigned to a carbonyl vibrational frequency, and the band at 1595 cm^{-1}

indicated the presence of an imine stretching frequency. A comparison of the spectra of the ligands and the metal complexes showed that there were shifts in the vibrational frequencies to a lower range, suggesting the formation of the complex. Likewise, the appearance of a new band in the fingerprint region at 529 cm^{-1} indicated an interaction of the metal with oxygen (M-O). A band at 484 cm^{-1} was assigned to the interaction of the metal and the nitrogen atom (M-N), which was absent in the spectrum of the ligand. This, therefore, served as an indication for the formation of the metal complex (Table 2).

The spectrum of Cu-L1-L2 showed a band at 3570 cm^{-1}, suggesting the presence of (O-H) water molecules. Broad bands at 3459 and 3280 cm^{-1} were indicative of the ν(N-H), a primary amine (Table 2). A weak band at 3160 cm^{-1} indicated the presence of ν(N-H) of a secondary amine. A medium intensity band at 1640 cm^{-1} suggested the presence of ν(C=O). The band at 1558 cm^{-1} indicated the presence of (C=N). The appearance of a new band at 544 cm^{-1} indicated metal-to-nitrogen (M-N) chelation and another band at 574 cm^{-1} was attributed to metal-oxygen (M-O) interaction, which was not present in the spectrum of the ligands.

In the spectrum of Cu-L1-L3, the weak band at 3507 cm^{-1} was attributed to the presence of the ν(O-H). Broad bands at 3459 and 3265 cm^{-1} ascribed to ν(N-H) of a primary amine (Table 2). The band at 3216 cm^{-1} indicated the presence of secondary amine. The bands at 2926 and 2855 cm^{-1} indicated the presence of the C-H vibrational frequency of 1,2-diaminocyclohexane. The (C=O) vibrational frequency was observed 1647 cm^{-1}. This suggests that a mixed ligand complex was obtained. It should be noted that such vibrational frequency was not observed bands do not exist in the spectrum of 1,2-diaminocyclohaxane. Furthermore, this band was observed at a higher frequency in relation to the free ligand. As a consequence, it was indicative of coordination of ligand L1 with the metal ion. The band at 1513 cm^{-1} indicated C=C of the aromatic ring, and the band at 1576 cm^{-1} indicated the presence of a C=N vibrational frequency. In the fingerprint region of the spectrum, the bands at 551 cm^{-1} and 624 cm^{-1} indicated the presence of Cu-N and Cu-O, respectively, indicating an interaction of nitrogen and oxygen atoms of the ligands with metal the metal ion.

Table 2: The relevant Infrared absorption band (cm^{-1}) of ligands and metal complexes

Complexes	1°ν(N-H)	2°(N-H)	ν(C=O)	ν(C=N)	ν(O-H)	ν(M-O)	ν(M-N)
Semicabazide	3425,3306	3239	1677	-	-	-	-
Benzaldehyde	-	-	1695	1595	-	-	-
L1	3280, 3246	3160	1643	1595	-	-	-
L2	-	-	1720	-	3497	-	-
L3	3354, 3280	-	-	-	-	-	-
Cu-L1	3455, 3283	3194	1640	1595	-	529	484
Ni-L1	3462, 3280	3242	1643	1595	-	484	428
Cu-L1-L2	3459, 3265	3216	1647	1576	3507	624	551
Ni-L1-L2	3455, 3280	3242	1643	1595	-	529	488
Cu-L1-L3	3459, 3265	3216	1647	1576	3507	624	551
Ni-L1-L3	3459, 3280	3160	1643	1595	-	506	424

Infrared Spectra of nickel (II) complexes

All of the nickel complexes followed similar trend in the formation of the complexes. In the spectrum of Ni-L1, Ni-L1-L2, and Ni-L1-L3, the broad bands at 3462-3242 cm^{-1} indicated the presence of a primary N-H vibrational frequency. The band located at 3242 cm^{-1} in Ni-L1-L2, and Ni-L1-L3 **(**Table 2) indicated secondary amine N-H vibrational frequency. This was observed at 3160 cm^{-1} in Ni-L1-L3. Comparing the ligand and the complexes, there are many similarities in vibrational frequency due to the nature of the environment. The nickel(II) complexes possessed diamagnetic properties, suggesting that all electrons are paired and have lower energies, resulting in possible vibration reduction during complex formation. Therefore, intensity of their bands decreased compared to the ligands. The appearance of new bands at 484 and 428 cm^{-1} indicated chelation of the metal to oxygen M-O and metal to nitrogen M-N vibrational frequencies in the Ni-L1. Similar to this, the bands at 529 and 488 cm^{-1} in Ni-L1-L2 indicated metal-oxygen and metal-nitrogen stretching frequencies and, thus, coordination (Table 2). This was observed at 506 and 424 cm^{-1}, respectively, for Ni-L1-L3.

Electronic absorption spectra and Magnetic susceptibility

Electronic Absorption Spectra of Ligands

The electronic spectra of benzaldehyde semicarbazone showed absorption bands at 209 and 283 nm. The bands correspond to $\pi \rightarrow \pi^*$ transition attributed to aromatic C=C and $n \rightarrow \pi^*$ transition attributed to νC=N and νC=O groups present in the ligand molecule. Electronic spectra of **L2** exhibited absorption bands at 234 and 275 nm, corresponding to $\pi \rightarrow \pi^*$ and $n \rightarrow \pi^*$ transition, respectively. The electronic spectrum of **L3** elicited bands at 202 and 324 nm ascribed to $n \rightarrow \sigma^*$ and $n \rightarrow \pi^*$ transitions, respectively (Table 3).

Electronic Absorption Spectrum and Magnetic Moment of Cu-L1

Electronic spectra of Cu-L1 showed two absorption bands at 209 nm and 278 nm in the ultraviolet region due to the $\pi \rightarrow \pi^*$ transition and the $n \rightarrow \pi^*$ transition of the chromophores with nonbonding electrons from the ligand (Table 3). The ligand-to-metal charge transfer band (LMCT)

observed at 417 nm can be assigned to the intraligand N$\rightarrow$Cu and O$\rightarrow$Cu charge transfer transitions, which is due to overlap by charge transfer in the visible region. A broad visible absorption band at 765 nm with a shoulder was observed. The shoulder band resulted from Jahn-Teller distortion that occurred during coordination. The broadband was assigned to the $^2E_g \rightarrow {}^2T_{2g}$ transition of the Cu^{2+} ion. Therefore, indicating an octahedral geometry with a six-membered ring for the synthesized complex. Due to the magnetic susceptibility obtained, the mass susceptibility value was negative, indicating that the complex is diamagnetic and also the magnetic moment of the complex was much smaller (0.50 BM) than the theoretically expected (1.73 BM) value. This suggests interaction or coupling between unpaired electrons of two copper atoms to form a dimeric complex.

Electronic Absorption Spectrum and Magnetic Moment of Cu-L1-L2

The electronic spectra of Cu-L1-L2 showed two absorption bands at 209 and 279 nm in the ultraviolet region due to $\pi \rightarrow \pi^*$ transition and $n \rightarrow \pi^*$ transition of chromophores with non-bonding electrons from the ligand (Table 3). The spectrum showed broad d-d bands in the region of 524-766 nm which can be assigned to $^2E_g \rightarrow {}^2T_{2g}$ transition of octahedral geometry. These bands indicated a Jahn-Teller distortion of octahedral system. From the magnetic susceptibility, the mass susceptibility of the complex is positive with the magnetic moment of 1.71 BM, indicating that the complex was paramagnetic and has an unpaired electron. Hence, suggesting the structure to be octahedral.

Electronic Absorption Spectrum and Magnetic Moment of Cu-L1-L3

The electronic spectra of Cu-L1-L3 showed two absorption bands at 214 and 278 nm in the ultraviolent region due to $\pi \rightarrow \pi^*$ transition of the aromatic ring and $n \rightarrow \pi^*$ transition of the C=N, C=O groups from the ligand (Table 3). The spectrum showed a broad d-d band at 761 nm, which can be assigned to $^2E_g \rightarrow {}^2T_{2g}$ transition of octahedral geometry. The spectrum showed more than one band, indicating a Jahn-Teller distortion of the octahedral system (Table 3). From the magnetic susceptibility of the complex, the value

of the mass susceptibility is positive, indicating paramagnetic property for the complex, but the value of the magnetic moment was lower (1.60 BM) than the theoretical value (1.73 BM), suggesting that there is an interaction or a coupling of the unpaired spins of two Cu^{2+} ion resulting in a low-lying singlet (diamagnetic properties).

Electronic Absorption Spectra and Magnetic Moment of Nickel(II) complexes
The electronic spectra of the nickel(II) complexes exhibited a similar trend with each other. The UV-Vis spectrum showed two absorption bands ranging from 204-213 nm and 280-279 nm in the ultraviolet region ascribed to $\pi \rightarrow \pi^*$ and $n \rightarrow \pi^*$ transitions, respectively (Table 3). LMCT bands were observed at 525, 410, and 478 nm for Ni-L1,

Ni-L1-L2, and Ni-L1-L3, respectively. This may be assigned to $N \rightarrow Ni$ and $O \rightarrow Ni$ charge transfer. This is due to the intensity charge transfer (CT) band. The spectrum of Ni-L1 exhibited bands at 709 and 764 nm. Similar bands were observed for Ni-L1-L2 and Cu-L1-L3 at 640, 761 and 620, 762 nm, respectively (Table 3). These were assigned as $A_{1g} \rightarrow {}^1A_{2g}$, ${}^1A_{1g} \rightarrow {}^1B_{1g}$ and ${}^1A_{1g} \rightarrow {}^1E_g$ transitions respectively. This supports a square planar geometry for the Ni(II) complexes. The magnetic susceptibility of the Ni^{2+} complexes also confirmed this geometry for the complexes. All the mass susceptibility of the nickel(II) complexes were negative (less than zero), which is indicative of the diamagnetic property of the complex. Therefore, this serves to confirm the square planar geometry for the nickel(II) complexes.

Table 3: The relevant electronic spectra and magnetic moments data.

Complex	Proposed Molecular weight (g/mol)	λ_{max} (nm)	Observed μ_{eff} (BM)
Cu-L1	815.806	209, 283	0.52
Ni-L1	385.032	209, 279, 766	0.66
Cu-L1-L2	549.963	234, 275	1.71
Ni-L1-L2	309.879	214, 278,764	0.40
Cu-L1-L3	713.783	206,279,420,768	1.64
Ni-L1-L3	334.020	212,280,425,714,765	0.41

From the results obtained, it is proposed that ligands **L1**, **L2** and **L3** coordinated in a bidentate fashion. Ligand **L1** made use of the oxygen atom of the carbonyl and the imine nitrogen atoms as donor atoms for coordination with the metal ion. Ligand **L2,** on the other hand, made use of an oxygen atom of both carboxylate ions in the molecule. The fact that the carboxylic acid moiety in **L2** was deprotonated prior to coordination is evidenced by the fact that the infrared spectrum of **L2** exhibited a band of 3497 cm^{-1} which was ascribed to the O-H stretching frequency in the free ligand. This was, however, absent in that of the coordinated ligand. In **L3** the two amino substituents were used in coordination, this is in agreement with previous reports (Aiyelabola, 2021). Evidence for the formation of mixed ligand complexes for the copper(II) complexes was provided from data obtained from the FTIR spectrum of the complexes. The spectrum of Cu-

L1-L2 exhibited vibrational frequencies at 1558, 1435, 1353 and 1259 cm$^{-1,}$ indicative of carboxylate ion stretching frequencies ascribed to (COO⁻) symmetric and asymmetric frequency bands. This supports the deprotonation of the carboxylic acid substituent in **L2** before coordination. It should be noted that these frequencies were absent in other copper(II) complexes. For Cu-L1-L3, a medium double spike was observed at 3265 and 3216 cm^{-1} and attributed to the ν(N-H) of the amino substituent in **L3.** In the case of the nickel(II) complexes, a clear distinction could not be readily made between the mixed ligand complexes and the traditional type of complexes. This has been attributed to the masking of such bands responsible for this. However, data obtained from the fingerprint region of the FTIR spectrum of these complexes suggest the coordination of the secondary ligands. In addition to this, evidence from the electronic

spectrum (in comparison with the traditional complexes), magnetic moment and percentage metal composition suggested the formation of the mixed ligand complexes for Ni-L1-L2 and Ni-L1-L3 as well. Therefore, based on the results obtained, a dimeric structure is proposed for complexes Cu-L1 and Cu-L1-L3. These are depicted in Figure 3 Similar structures have been shown for some copper(II) carboxylates and green copper(II) acetate (Greenwood and Hernshaw). The magnetic moment obtained for both complexes indicated Cu-Cu interaction (coupling) with possible super exchange between the central metal ions (Aiyelabola *et al*., 2017). On the other hand, an octahedral geometry is proposed for Cu-L1-L2, which is illustrated in Figure 3. Interestingly enough, based on the results obtained, square planar geometry is proposed for the nickel(II) complexes and is represented in Figure 3.
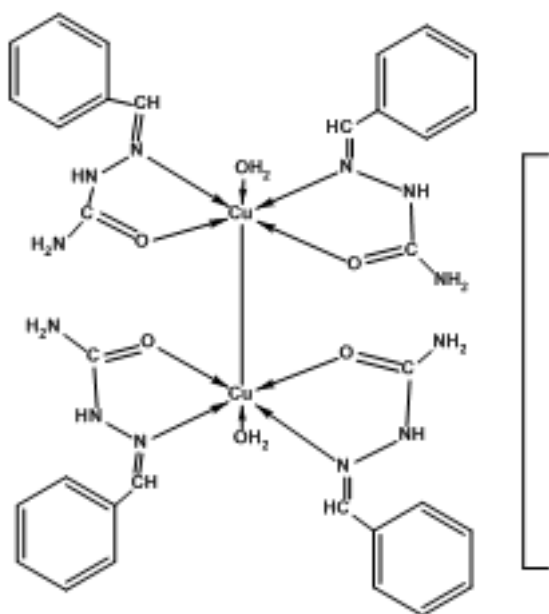
Cu-L1 = $[Cu(L1)_2(H_2O)]_2$
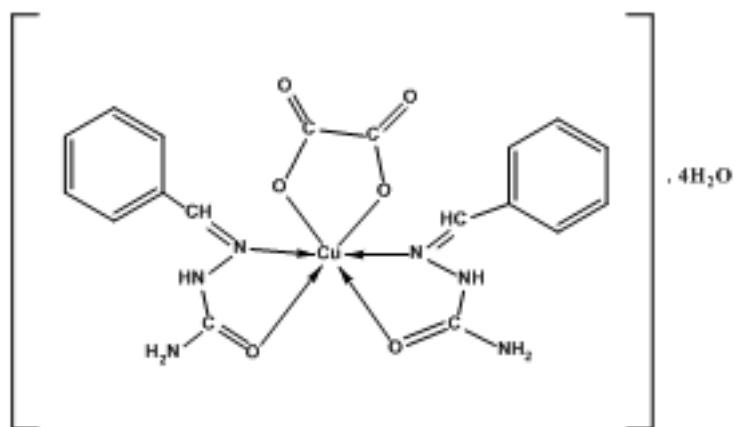
Cu-L1-L2 = $Cu(L1)_2L2.4H_2O$
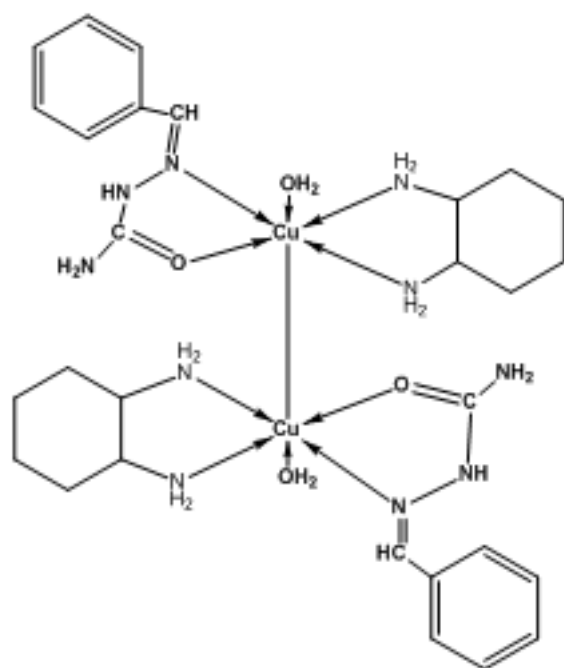
Cu-L1-L3 = $[Cu(L1)(L3)H_2O]_2$

Ni-L1 = $Ni(L1)_2$

Ni-L1-L2 = Ni(L1)(L2)   **Ni-L1-L3**= [Ni(L1)(L3)]
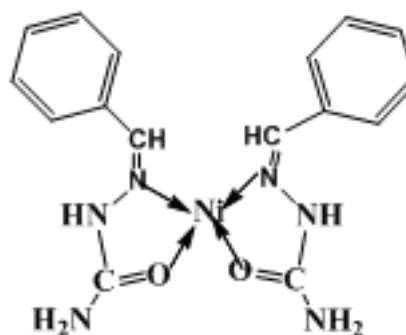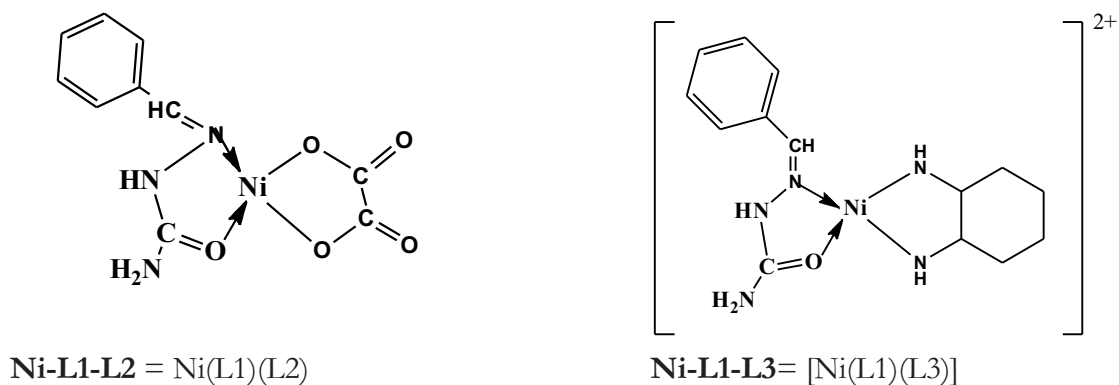
Figure 3: The proposed structures of the synthesized complexes after analysis of IR data, electronic absorption and magnetic moment.

In-silico **DNA Binding Studies**

Docking studies were performed with the software program AutoDock 4.2 to determine the binding interactions of the complexes towards the synthetic bDNA (1BNA) as a model for ct-DNA. The docking result obtained by the AutoDock program after performing the calculations gave estimates of the binding affinity of each complex, as shown in Table 5. All values obtained from the results were negative, indicating that binding had occurred between the DNA and the complexes. The only exception was Cu-L1, whose binding affinity was found to be positive, indicating that no binding occurred. Cu-L1-L3 had the most negative binding affinity, suggesting higher binding potential and the possibility of stronger interactions that could lead to inhibition. The 2D and 3D interactions of the docking results were determined using a combination of programs, PyMol and Discovery Studio Visualizer which facilitated the identification of significant interactions (Figures 4-9) between the synthesized complexes and the DNA binding sites (Table 4). Based on the obtained results, it was found that there are various interactions between the synthesized complexes and the DNA. It has been observed that these hydrophobic (π-π, π-donor hydrogen) interactions and hydrogen bonding (conventional and carbon-hydrogen bonds) comprise the most common and important type of interaction of all complexes studied. Overall, all interactions and binding affinities are considered. Considering this, Cu-L1-L3 had the highest binding affinity compared to all other complexes. All the complexes docked with the

bDNA had higher binding affinity compared to the reference compound (oxaliplatin, one of the chemotherapy agents used for the treatment of breast cancer), except Cu-L1-L2; it is suggested that this may be as a result of the kind of interactions that occurred when binding with bDNA. It is worth noting as well that Cu-L1-L3 had the most polar interactions, which might have contributed to its higher binding affinity relative to the other complexes. It was also observed that the aromatic systems in the bDNA surrounding the metal complexes contributed immensely to the hydrophobic interactions, which might have contributed to the stability of the overall complex, that is, the complex of DNA with study complexes (extensive hydrophobic interactions were observed).

In the case of Cu-L1-L2, the L2 (oxalate ion) was removed prior to the molecular docking exercise due to the fact that the known metal complexes that have the oxalate bound do not usually make it to the target in biological systems. This is because the oxalate ion is a leaving group which is displaced as a stable species, taking with it the bonding electrons (Mehmood, 2014). This is typified by the mechanism of action of cisplatin and oxaliplatin in which the oxalate ions were displaced as well. Hence, it is usually assumed that the complex without the bound oxalate is what is responsible for the observed biological activity that is a function of DNA binding and intercalation, thus warranting the reduction of Cu-L1-L2 and Ni-L1-L2 by the removal of oxalate ion prior to docking exercise leaving Cu-L1 and

Table 4: Molecular Docking Parameters for 1BNA Interaction with Metal Complexes

Complex	Internal energy (kcalmol^{-1})	Interacting bases	Polar Contact	Hydrogen bond length (A)	Description of hydrogen bonds (H-bonds)
CuL1	+22.85				
CuL1L2	-4.56	DC-3, DT-20	2	3.2	N-H of semicarbazone and phosphate of cytosine DC-3
				3.0	Aromatic ring of semicarbazone and hetero aromatic ring of thymine DT-20
CuL1L3	-7.96	DA-5, DG-4, DG-16, DA-5, DA-17, DA-18, Da-5, DA-18	7	3.4	C-H of cyclohexane diamine and aromatic ring of adenine DA-5
				2.9	Aromatic ring of semicarbazone and hetero aromatic ring of ganine DG-4, DG-16
				2.6	N of semicarbazone and N-H of adenine DA-5, DA-18
				2.5	N-H of semicarbazone and hetero aromatic ring of adenine DA-17
					N-H of semicarbazone and N of adenine DA-18
NiL1	-6.67	DG-16, DA-17, DA-6, DA-5	4	3.5	N-H of semicarbazone and hetero aromatic ring of guanine DG-16
				3.0	N-H of semicarbazone and hetero aromatic ring of adenine DA-17
					Aromatic ring of semicarbazone and adenine DA-6, DA-5
NiL1L2	-6.56	DC-9, DT-19, DT-18, DT-19, DC-19	5	3.5	N of semicarbazone and sugar ribose of cytosine DC-9
				3.2	N of semicarbazone and phosphate of thymine DT-19
				3.0	N-H of semicarbazone and N of adenine DA-18
				2.9	O of semicarbazone and phosphate of thymine DT-19
					N of semicarbazone and sugar ribose of cytosine DC-19

NiL1L3	-6.02	DA-A5, DA-A5, DA-17, DA6, DA-5, DA-5	6	2.5	N-H of semicarbazone and phosphate of adenine DA-5
				3.3	Aromatic ring of semicarbazone and N of adenine DA-17
					Cyclohexane ring and N-H of adenine DA-5
					Cyclohexane ring and aromatic ring of adenine DA-5
					N-H of cyclohexane diamine and phosphate of adenine DA-6
					Ni ion and phosphate of adenine DA-5
oxaliplatin	-5.30	DA-18, DT-8	2	3.2	N-H of cyclohexane diamine and O atom of thymine DT-8
				2.9	N-H of cyclohexane diamine and N of adenine DA-18
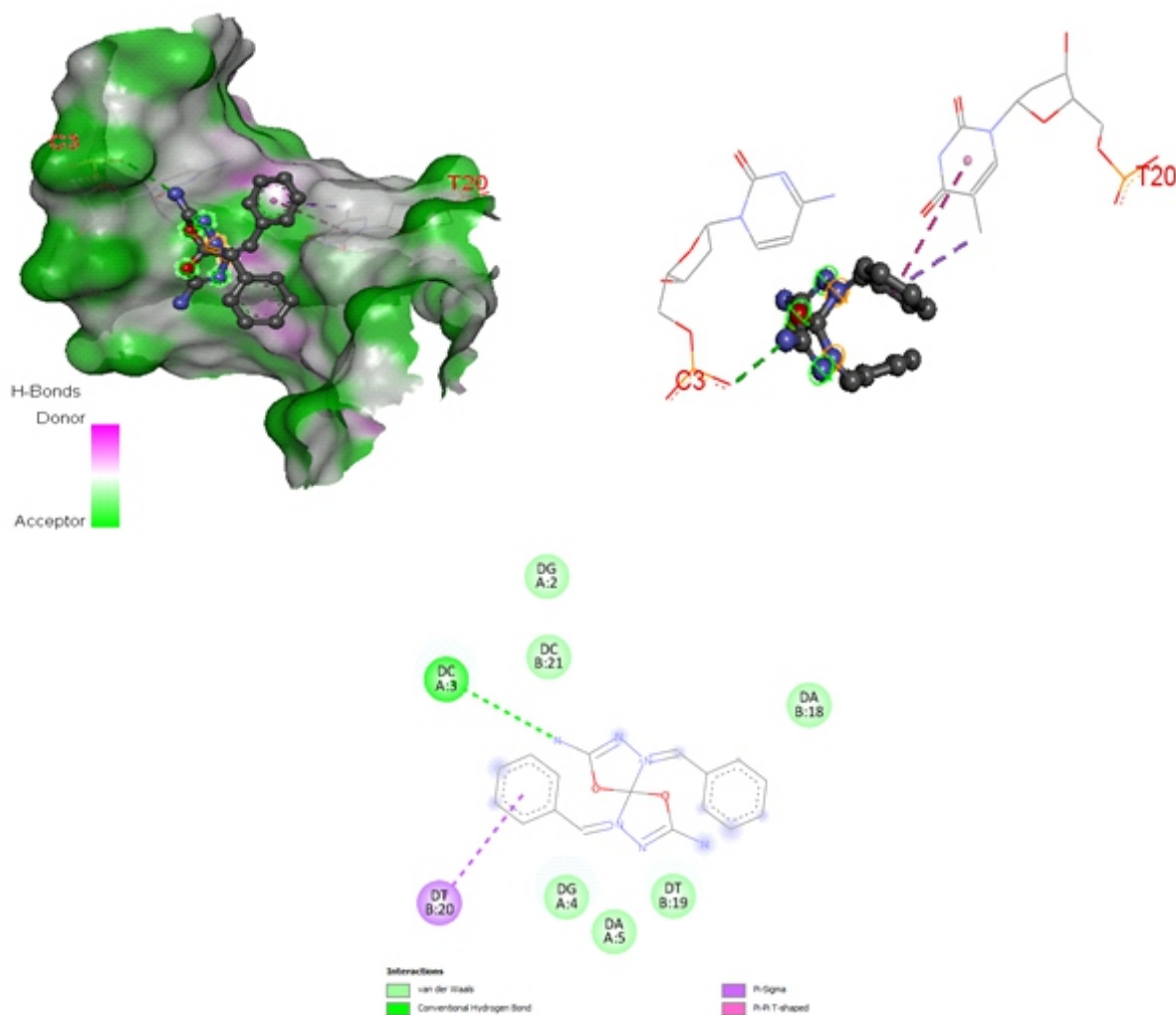
Figure 4: 2D and 3D Visualization of B-DNA (PDB ID: 1BNA) complexed with Cu-L1-L2 CuL1-L2 (reduced to Cu-L1) and pose within a major groove.
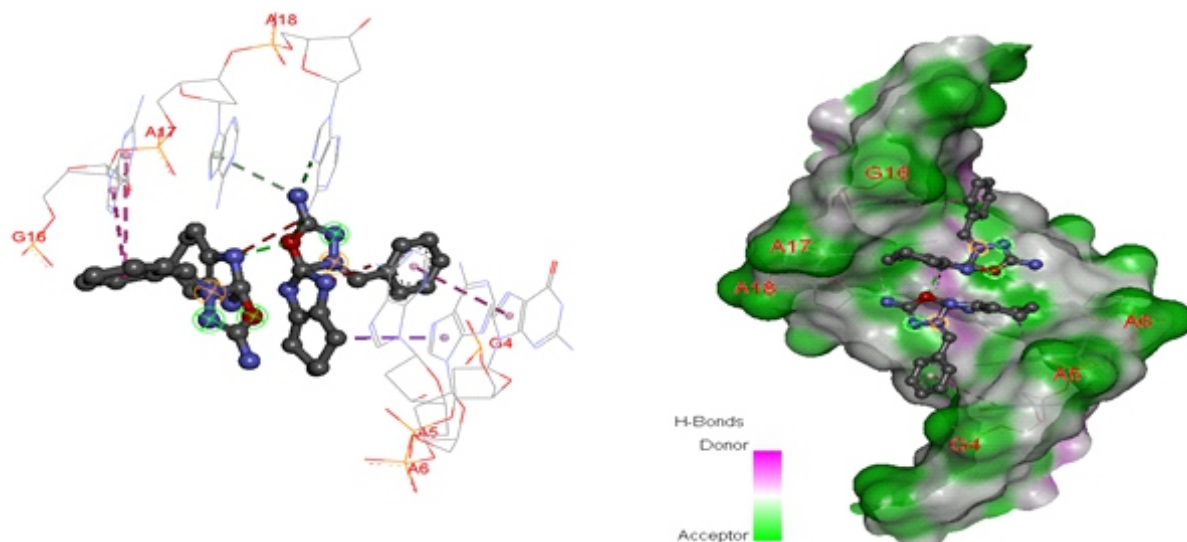
Figure 5: 3D Visualization of B-DNA (PDB ID: 1BNA) with Cu-L1-L3 and pose within major groove
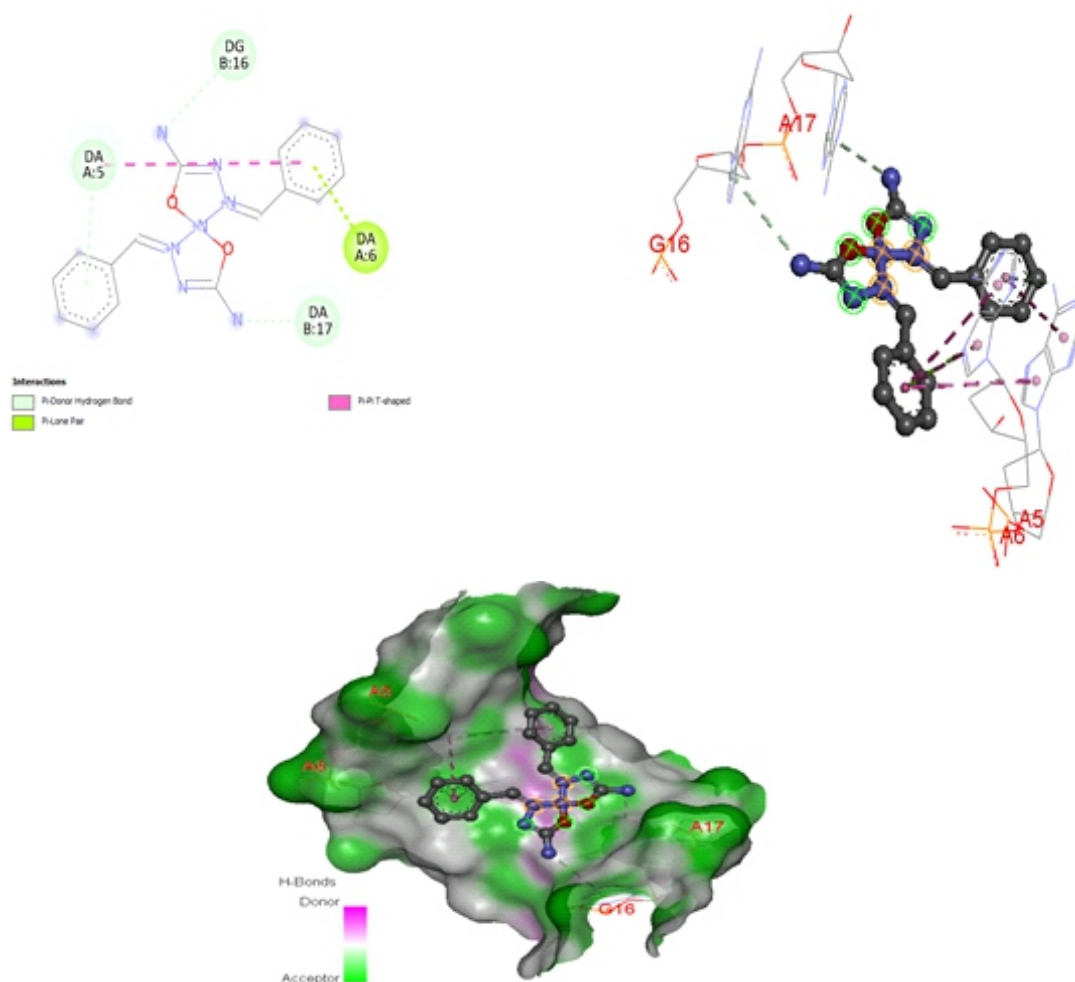
Figure 6: 2D and 3D Visualization of B-DNA (PDB ID: 1BNA) with Ni-L1-L1 and pose within a major groove
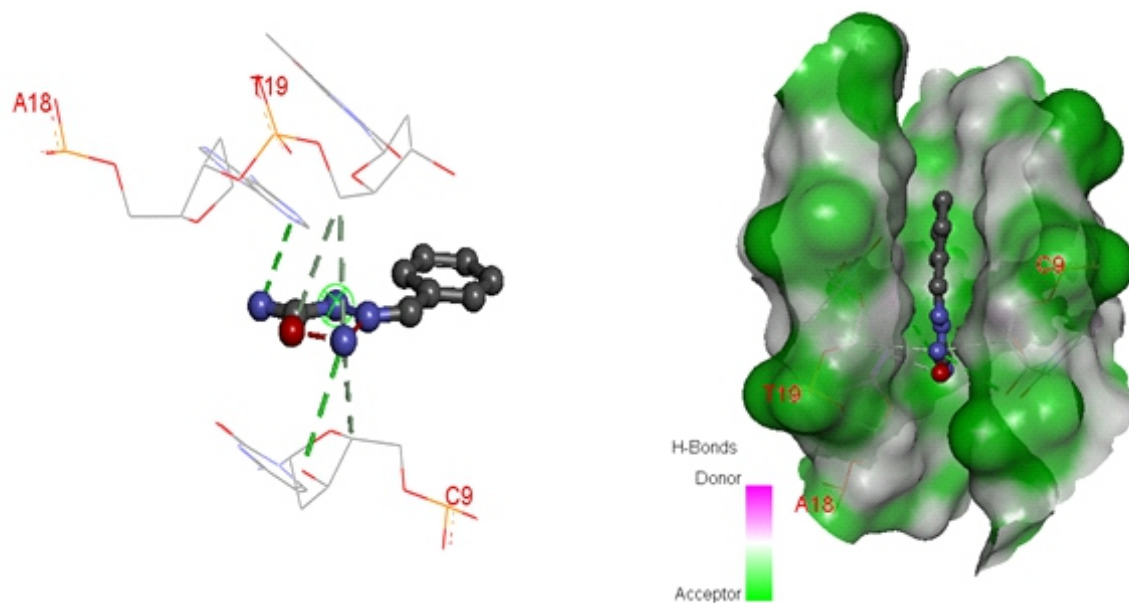
Figure 7: 3D Visualization of B-DNA (PDB ID: 1BNA) with Ni-L1-L2 (reduced to Ni-L1) and pose within a minor groove
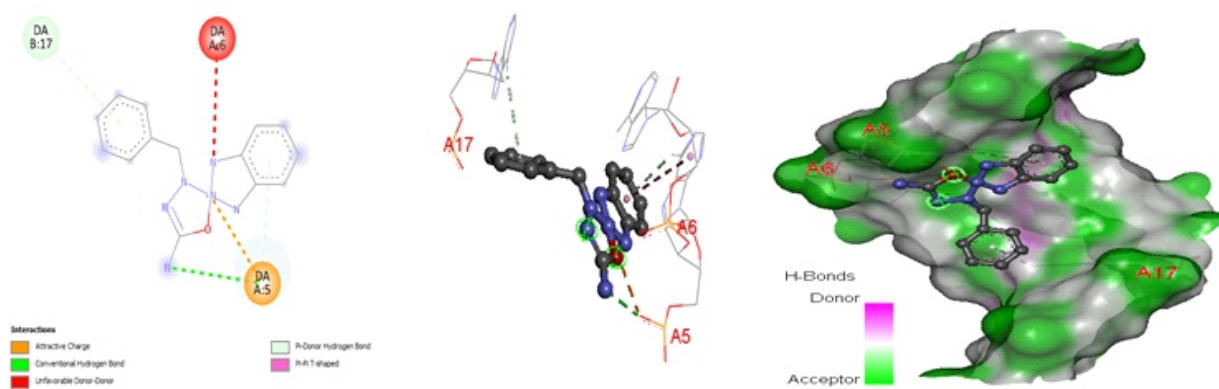
Figure 8: 2D and 3D Visualization of B-DNA (PDB ID: 1BNA) with Ni-L1-L3 and pose within a major groove.
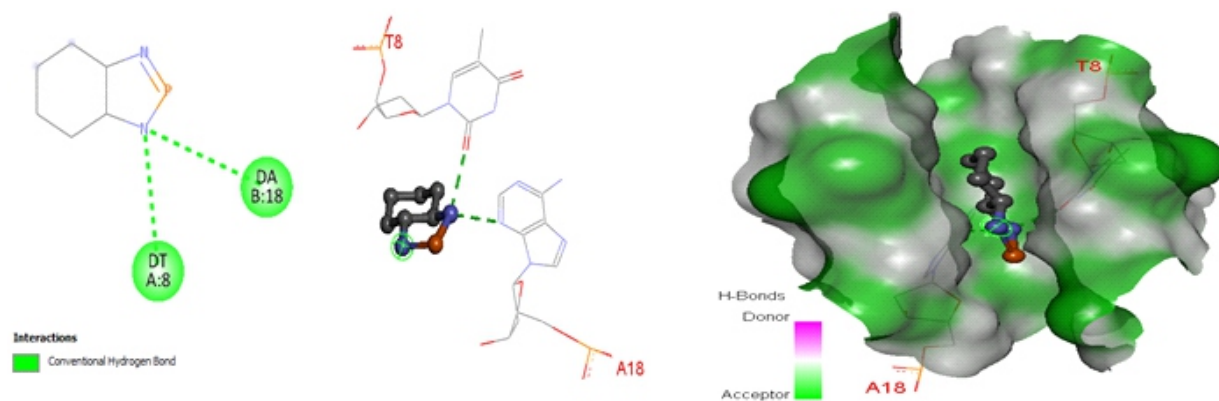
Figure 9: 2D and 3D Visualization of B-DNA (PDB ID: 1BNA) with NiL1L3 and Grooving mode

In vitro cytotoxic studies

In vitro cytotoxicity studies of the complexes, including the control, were analyzed against brine shrimp nauplii using the lethality assay commonly used for *in vitro* cytotoxicity studies (Waghulde *et al*., 2019). Five concentrations of each complex (200, 400, 600, 800 and 1000 g/ml) were treated with the *Artemia nauplii*. LC_{50} viability is given in Table 5. From the results obtained, all the synthesized complexes exhibited significant cytotoxic effects. This is because, generally, complexes with LC_{50} values below 1000 µg/ml have the potential to be good cytotoxic agents. Also, the synthesized metal complexes showed a significant value of less than 0.05 (5% error probability during the analysis), indicating that the concentration of the synthesized complexes is significant on each value (Waghulde *et al*., 2019). Comparing all synthesized metal complexes, Cu-L1-L2 and Cu-L1-L3 exhibited the strongest cytotoxic effect with the lowest LC_{50} values.

Complexes of copper are expected to be more toxic than that of nickel based on information available in literature concerning the effects of copper relative to that of nickel (Goodman *et al*., 2016). However, a comparison of the result obtained from the preliminary screening on cytotoxicity of the synthesized metal complexes with the result obtained from molecular docking with DNA (Table 5), showed that the cytotoxicity effect of CuL1L1 was less compared to the cyctotoxic effect expected from copper complexes (Rogala *et al*., 2022) and the docking calculation showed that the binding affinity was positive (which implies that binding did not occur between the complex and the DNA). It can be said that since there was no binding with the DNA, there is a possibility that the particular metal complex would have a low cytotoxic effect in the test subjects (brine shrimp nauplii). Hence, this indicated that it is possible that the effect of cytotoxicity may be associated with the binding of the metal complexes to the DNA. The result from the preliminary screening on cytotoxicity of CuL1L2 and CuL1L3 showed that they have high cytotoxicity effect which correlates with the observed high binding affinities and corroborate the fact that the cytotoxicity in the brine shrimp is a function of DNA binding.

Table 5: LC_{50} cytotoxicity values and docking data of the complexes

Complexes	Internal energy (kcalmol^{-1})	Number of polar interactions	Cytotoxicity level [LC_{50} (µg/ml)]
Cu-L1	+22.85	-	719.17
Ni-L1	-6.67	2	804.96
Cu-L1-L2	-4.56	2	224.07
Ni-L1-L2	-6.56	2	619.88
Cu-L1-L3	-7.96	4	227.73
Ni-L1-L3	-6.02	2	681.09

CONCLUSION

In the present study, (*E*)-2-benzylidene-hydrazinecarboxamide and its metal complexes were synthesized and analyzed by spectral measurement, physio-chemical (melting point measurement, metal analysis, solubility test), and magnetic moment. The brine shrimp lethality assay was carried out on the metal complexes, and the *in-silico* studies on DNA binding ability were carried out. The spectral results suggested octahedral geometry for all the copper complexes where two out of the three copper complexes are dimers (Cu-Cu); the spectral results for all nickel complexes suggest square planar geometry with diamagnetic properties.

Based on the information obtained from the preliminary screening on cytotoxicity and the docking conformation, it can also be concluded that nickel(II) complexes were not as toxic as the copper(II) complexes. The presence of (*E*)-2-benzylidenehydrazinecarboxamide had shown a

large effect on the complexes which interacted and bound most with the DNA via the heterocyclic aromatic ring. This suggests its potential usage with respect to this mechanism of activity. Correlating the results obtained from the cytotoxicity analysis with data from molecular docking indicated that the copper complex, Cu-L1**,** that did not bind with B-DNA in the docking exercise showed a less cytotoxic effect. This implies that the binding of the metal complex may be critical for the mechanism of their activity as potential anticancer agents. The other two copper complexes (Cu-L1-L2 and Cu-L1-L3) that bound to the DNA appeared to have a significant cytotoxic effect. Cu-L1-L3 had the most interaction and binding affinity to B-DNA, better than oxaliplatin, a well-established line of treatment for breast cancer. This, therefore, shows its potential anticancer property, such as the platinum-based drugs, with the additional plausible less side effect contrary to what obtains for the platinum-based complexes. Hence, suggesting it for further consideration as an anticancer agent for the treatment of breast cancer.

REFERENCES

Aiyelabola T., Akinkunmi E., Obuotor E., Olawuni I., Isabirye D. and Jordaan J. (2017) Synthesis Characterization and Biological Activities of Coordination Compounds of 4-Hydroxy-3-nitro-2*H*-chromen-2-one and Its Aminoethanoic Acid and Pyrrolidine-2-carboxylic Acid Mixed Ligand Complexes Bioinorganic Chemistry and Applications 1- 9

Aiyelabola, T.O., Otto, D.P., Jordaan, J.H.L., Akinkunmi, E.O. and Olawuni, I. (2021) Synthesis, Characterization, Antimicrobial and DNA Binding Studies of a Tetradentate N_2O_2 Amino Acid Schiff Base and Its Coordination Compounds. *Advances in Biological Chemistry*, 11, 30-51.
doi: 10.4236/abc.2021.111004

Aiyelabola, T.O. (2021). Syntheses, Characterization and Biological Activity of Coordination Compounds of 3-Hydroxy-2-methyl-4*H*-pyran-4-one and Its Mixed Ligand Complexes with 1,2-Diaminocyclohexane *Advances in Biological Chemistry*, 11, 106-112.

Dhabale, R. H., Shah, S., Tiwari, N., & Patani, P. (2022). Review of Semicarbazone, Thiosemicarbazone, And Their Transition Metal Complexes, And Their Biological Activities. *Journal of Pharmaceutical Negative Results*, 2416-2424.
doi: 10.47750/pnr.2022.13.S05.377

Đuri, S.Z., Vojnovic, S., Andrejevi, T.P., Stevanovi, N.L., Savi, N., Nikodinovic-Runic, J., *et al.* (2020). Antimicrobial Activity and DNA/BSA Binding Affinity of Polynuclear Silver(I) Complexes with 1,2-Bis(4-pyridyl)ethane/ethene as Bridging Ligands. *Bioinorganic Chemistry and Application*s, Article ID: 3812050.
doi: 10.1155/2020/3812050

Feng, Y., Spezia, M., Huang, S., Yuan, C., Zeng, Z., Zhang, L., and Ren, G. (2018). Breast cancer development and progression: Risk factors, cancer stem cells, signaling pathways, genomics, and molecular pathogenesis. *Genes & diseases*, 5(2), 77-106.
doi: 10.1016/j.gendis.2018.05.001

Florea, A. M., and Büsselberg, D. (2011). Cisplatin as an anti-tumor drug: cellular mechanisms of activity, drug resistance and induced side effects. *Cancers*, 3(1), 1351-1371.
doi: 10.3390/cancers3011351

Icsel, C., Yilmaz, V. T., Aydinlik, Ş., & Aygun, M. (2020). New manganese (II), iron (II), cobalt (II), nickel (II) and copper (II) saccharinate complexes of 2, 6-bis (2-benzimidazolyl) pyridine as potential anticancer agents. *European Journal of Medicinal Chemistry*, 202, 112535.
doi: 10.1016/j.ejmech.2020.112535

Martínez-Gutierrez, F., Thi, E. P., Silverman, J. M., de Oliveira, C. C., Svensson, S. L., Hoek, A. V., and Bach, H. (2012). Antibacterial activity, inflammatory response, coagulation and cytotoxicity effects of silver nanoparticles. *Nanomedicine: Nanotechnology, Biology and Medicine*, *8*(3), 328-336.
doi: 10.1016/j.nano.2011.06.014

Mehmood, R. K. (2014). Review of Cisplatin and oxaliplatin in current immunogenic and monoclonal antibody treatments. *Oncology reviews*, 8(2), 36-43.

Shobha Devi, C., Thulasiram, B., Aerva, R. R., and Nagababu, P. (2018). Recent advances in copper intercalators as anticancer agents. *Journal of Fluorescence*, *28*, 1195-1205.
doi: 10.1007/s10895-018-2283-7

Tamasi, G., Serinelli, F., Consumi, M., Magnani, A., Casolaro, M., & Cini, R. (2008). Release studies from smart hydrogels as carriers for piroxicam and copper(II)–oxicam complexes as anti-inflammatory and anti-cancer drugs. X-ray structures of new copper (II)–piroxicam and–isoxicam complex molecules. *Journal of inorganic biochemistry*, *102*(10), 1862-1873.
doi: 10.1016/j.jinorgbio.2008.06.009

Wende, C., Lüdtke, C., and Kulak, N. (2014). Copper Complexes of N-Donor Ligands as Artificial Nucleases. *European Journal of Inorganic Chemistry*, *2014*(16), 2597-2612.
doi: 10.1002/ejic.201400032

Wilfredo, H., and Juan, P. (2006). Complexes of Semicarbazone and Thiosemicarbazone. *Journal of Chemical science*, *14*, 10-20.
doi: 10.47750/pnr.2022.13. S05.377

Zubair, M., Khalil, S., Rasul, I., Nadeem, H., Noor, F., Ahmad, S., and Alshehri, Z. S. (2023). Integrated molecular modeling and dynamics approaches revealed potential natural inhibitors of NF-$\varkappa$B transcription factor as breast cancer therapeutics. *Journal of Biomolecular Structure and Dynamics*, 1-15.
doi: 10.1080/07391102.2023.2214209